AI-Driven RSMA Beamforming for Integrated Sensing and Communication in Terrestrial-Satellite Networks

Mario R. Camana[1], Carla E. Garcia[1], Konstantinos Ntontin[1], Khalid Qaraqe[2], and Symeon Chatzinotas[1]
[1]*Interdisciplinary Centre for Security, Reliability and Trust, University of Luxembourg, 4365 Luxembourg City, Luxembourg*
[2]*College of Science and Engineering, Hamad Bin Khalifa University, Doha, Qatar*
Email: {mario.camana, carla.garcia, kostantinos.ntontin}@uni.lu, kqaraqe@hbku.edu.qa, symeon.chatzinotas@uni.lu.

***Abstract*—The increasing demand for high-capacity and globally accessible wireless services has intensified the need for spectrum-efficient and wide-coverage solutions. Integrated terrestrial-satellite networks (ITSNs) offer a promising architecture to address these challenges, while with the deployment of integrated sensing and communication (ISAC) and rate-splitting multiple access (RSMA) further enhances system functionality by supporting joint communication and sensing while effectively managing interference. This paper investigates RSMA for a multi-antenna LEO satellite that shares the licensed spectrum of terrestrial distributed MIMO systems to simultaneously perform target sensing and provide communication services. A weighted sum-rate maximization problem is formulated, subject to power, sensing, and interference constraints. To solve the resulting non-convex problem, we develop a hybrid solution that combines a deep convolutional neural network (CNN) for power allocation with a semidefinite relaxation (SDR)-based method for precoding and rate optimization. Simulation results demonstrate that the proposed scheme satisfies all constraints and achieves performance close to a successive convex approximation (SCA)-based benchmark, while significantly reducing computational time, which makes it suitable for real-time deployment in resource-constrained satellite systems. Additionally, the RSMA-based approach outperforms conventional baseline methods.**

***Index Terms*—Integrated terrestrial-satellite networks, distributed MIMO, rate-splitting multiple access (RSMA), integrated sensing and communication (ISAC), artificial intelligence (AI).**

I. Introduction

The exponential growth in wireless data traffic, driven by multimedia services and bandwidth-intensive applications, has intensified spectrum scarcity. Concurrently, achieving global wireless coverage remains constrained by the high cost and logistical complexity of deploying terrestrial infrastructure in remote regions. These challenges highlight the need for solutions that enhance spectrum efficiency and extend coverage. Integrated terrestrial–satellite networks (ITSNs) offer a promising architecture to address these issues by enabling spectral coexistence between terrestrial and satellite systems, thereby improving both spectral and energy efficiency across diverse geographical areas [1]. Their performance can be further enhanced with distributed multiple-input multiple-output (MIMO) in the terrestrial network, which mitigates inter-cell interference through distributed access points that cooperatively serve users, improving service uniformity and system capacity [2], [3]. These capabilities are especially beneficial in complex environments with distributed devices, where maintaining reliable connectivity and efficient spectrum utilization is challenging.

The deployment of integrated sensing and communication (ISAC) adds further value by enabling dual use of wireless signals for communication and sensing [4]. ISAC improves spectral efficiency, reduces hardware redundancy, and enables applications such as environmental monitoring, drone tracking, and remote sensing. Rate-splitting multiple access (RSMA) complements ISAC by managing interference and leveraging common messages for sensing, eliminating the need for dedicated radar signals [5], [6]. This makes RSMA particularly suitable for ITSNs, where efficient resource use and interference mitigation are critical.

Several studies have explored ISAC-enabled beamforming and resource allocation in terrestrial [4] and satellite networks [7]. The integration of ISAC into satellite–terrestrial relay networks has been considered in [8], where user activity sensing is employed to support a dynamic bandwidth allocation framework. This approach aims to enhance random access performance and maximize overall system throughput, underscoring the potential of ISAC to improve network adaptability and efficiency. In [9], the authors investigated a reconfigurable intelligent surface (RIS)-assisted ISAC-enabled ITSN in a single-cell scenario, focusing on sum-rate maximization. However, these works did not incorporate RSMA.

RSMA has been studied across various domains, including terrestrial networks [5], distributed MIMO systems [10], ISAC systems [6], and LEO-ISAC system [7]. These studies consistently demonstrate RSMA's superiority over conventional multiple access schemes in terms of spectral and energy efficiency. Nevertheless, prior works of ISAC and RSMA [4]–[10] primarily focus on terrestrial, satellite, or single-cell scenarios and do not investigate the joint integration of RSMA and ISAC within ITSNs incorporating terrestrial distributed

This work was supported by the project sElf-evolving terrestrial/nonTerrestrial Hybrid nEtwoRks (ETHER). The ETHER Project was supported by the Smart Networks and Services Joint Undertaking (SNS JU) through the European Union's Horizon Europe Research and Innovation Programme under Grant 101096526.

MIMO networks.

The practical deployment of joint communication and sensing systems faces significant challenges due to the complexity of their joint optimization. Traditional optimization methods are computationally intensive and struggle to adapt to dynamic channel conditions. AI-based approaches, particularly deep learning (DL), offer a promising alternative by learning system dynamics and enabling real-time adaptation of beamforming and resource allocation strategies. For instance, [11] proposed a deep convolutional linear precoder neural network for RSMA-based aerial computing networks, demonstrating the potential of DL in managing interference and improving spectral efficiency. Similarly, [9] introduced a deep Q-network for sum-rate maximization in ISAC-enabled ITSNs. However, this work did not include a feasibility analysis or a comparison with upper-bound benchmark schemes, leaving open questions regarding its practical performance and optimality.

Motivated by these insights, our work addresses the gap in the joint integration of RSMA and ISAC within satellite–terrestrial architectures, particularly under cognitive radio constraints and in distributed MIMO networks. To this end, we propose a novel AI-driven beamforming framework that enables efficient resource allocation and interference management. The proposed system model involves a LEO satellite interacting with a terrestrial distributed MIMO system to perform simultaneous sensing and communication using RSMA. Our objective is to maximize the system sum rate while satisfying power, interference, and sensing constraints. The main contributions can be summarized as follows:

- We propose a cognitive satellite–terrestrial network architecture in which a multi-antenna LEO satellite shares the licensed spectrum of a terrestrial distributed MIMO system to simultaneously perform target sensing and provide communication services to satellite users using RSMA. The spectrum sharing mechanism is designed to ensure that satellite transmissions do not exceed an interference threshold for terrestrial operations.
- We formulate a weighted sum-rate maximization problem by jointly optimizing the common precoder vector, common rate variables, and power allocation to satellite users subject to constraints on satellite power, minimum beampattern gain toward the sensing target, and maximum interference to terrestrial users. To solve the resulting non-convex problem, we propose a hybrid solution that combines a deep convolutional neural network (CNN)-based model for power allocation with a semidefinite relaxation (SDR)-based method for common precoding and rate optimization.
- Numerical simulations demonstrate that the proposed scheme satisfies all constraints and achieves performance close to the near-optimal successive convex approximation (SCA)-based benchmark, while significantly reducing computational time. Additionally, the RSMA-based approach outperforms conventional maximum ratio transmission (MRT) and zero-forcing (ZF) precoding.

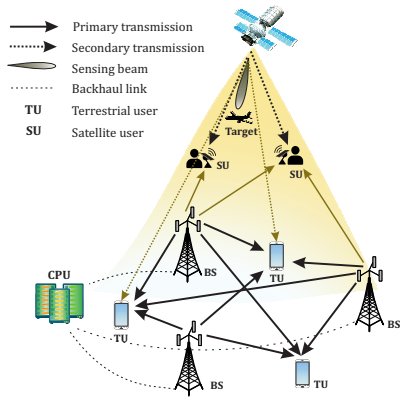

Fig. 1: ISAC-enabled integrated satellite and terrestrial distributed MIMO system.

II. System Model

We consider a LEO satellite with N antennas serving K satellite users (SUs) and performing sensing toward a target, as illustrated in Fig. 1. The terrestrial network includes B base stations (BSs), each with N_B antennas, and M terrestrial users (TUs). Each BS serves all TUs over the same time-frequency resource block, coordinated by a central processing unit (CPU) via backhaul links. We use underlay cognitive radio to enable the satellite system to share the licensed spectrum of terrestrial networks while ensuring that interference to terrestrial operations remains below a defined threshold.

Under RSMA at the satellite, each user message m_k is split into a common part m_k^c and a private part m_k^p. The common parts are jointly encoded into a common stream s_0, which is intended to be decoded by all users. Meanwhile, the private parts are independently encoded into private streams s_k. Linear precoding is then applied to all streams, where $\mathbf{p}_0$ denotes the common precoder for s_0, and $\mathbf{p}_k$ denotes the private precoder for for s_k. It has been shown that the common stream in RSMA can be exploited for sensing purposes, effectively replacing the need for a dedicated radar signal [6]. Accordingly, the transmit signal at the satellite is denoted as

$$\mathbf{x}_S = \mathbf{p}_0 s_0 + \sum_{k=1}^{K} \mathbf{p}_k s_k. \tag{1}$$

In the terrestrial network, we assume that the BSs employ local zero-forcing precoding to transmit the stream s_m^{TU} to the m-th TU. Then, the transmit signal at the b-th BS is given by

$$\mathbf{x}_{BS,b} = \sum_{m=1}^{M} \sqrt{q_{b,m}} \mathbf{w}_{T,b,m} s_m^{TU}, \tag{2}$$

where $q_{b,m}$ denotes the power allocated to the m-th TU at the b-th BS, and $\mathbf{w}_{T,b,m}$ is the corresponding precoding vector. The precoding matrix at the b-th BS is given by $\mathbf{W}_{T,b} = [\mathbf{w}_{T,b,1}, ..., \mathbf{w}_{T,b,M}] = \left[\frac{\tilde{\mathbf{w}}_{T,b,1}}{\|\tilde{\mathbf{w}}_{T,b,1}\|}, ..., \frac{\tilde{\mathbf{w}}_{T,b,M}}{\|\tilde{\mathbf{w}}_{T,b,M}\|}\right]$, where $\tilde{\mathbf{W}}_{T,b} = [\tilde{\mathbf{w}}_{T,b,1}, ..., \tilde{\mathbf{w}}_{T,b,M}] = \mathbf{G}_{T,b}\left(\mathbf{G}_{T,b}^H \mathbf{G}_{T,b}\right)^{-1}$ and $\mathbf{G}_{T,b} = [\mathbf{g}_{T,b,1}, ..., \mathbf{g}_{T,b,M}] \in \mathbb{C}^{N_B \times M}$ with $\mathbf{g}_{T,b,m} \in$

$\mathbb{C}^{N_B \times 1}$ representing the channel vector from the b-th BS to the m-th TU.

In the satellite network, the received signal at the k-th SU is given by

$$\begin{aligned} y_k =& \mathbf{h}_{S,k}^H \mathbf{p}_0 s_0 + \sum_{k'=1}^{K} \mathbf{h}_{S,k}^H \mathbf{p}_{k'} s_{k'} \\ &+ \sum_{b=1}^{B} \sum_{m=1}^{M} \mathbf{g}_{S,b,k}^H \sqrt{q_{b,m}} \mathbf{w}_{T,b,m} s_m^{TU} + n_k, \end{aligned} \tag{3}$$

where $\mathbf{g}_{S,k} \in \mathbb{C}^{N \times 1}$ denotes the channel from the satellite to the k-th SU, $\mathbf{g}_{S,b,k} \in \mathbb{C}^{N_B \times 1}$ represents the channel from the b-th terrestrial BS to the k-th SU, and n_k denotes the additive white Gaussian noise with zero mean and variance σ_k^2. We assume perfect channel state information (CSI), and discussions on imperfect CSI can be found in [12]. Each k-th SU first decodes the common stream s_0 by treating all private streams as noise. Then, the signal-to-interference-and-noise-ratio (SINR) of s_0 at the k-th SU is given by

$$\gamma_k^c = \frac{\left|\mathbf{h}_{S,k}^H \mathbf{p}_0\right|^2}{\sum\limits_{k'=1}^{K} \left|\mathbf{h}_{S,k}^H \mathbf{p}_{k'}\right|^2 + \sum\limits_{b=1}^{B} \sum\limits_{m=1}^{M} q_{b,m} \left|\mathbf{g}_{S,b,k}^H \mathbf{w}_{T,b,m}\right|^2 + \sigma_k^2}. \tag{4}$$

Next, the k-th SU applies successive interference cancellation (SIC) to remove the interference from the common message and then decodes its private stream. Hence, the SINR of s_k at the k-th SU is expressed as

$$\gamma_k^p = \frac{\left|\mathbf{h}_{S,k}^H \mathbf{p}_k\right|^2}{\sum\limits_{\substack{k'=1 \\ k' \neq k}}^{K} \left|\mathbf{h}_{S,k}^H \mathbf{p}_{k'}\right|^2 + \sum\limits_{b=1}^{B} \sum\limits_{m=1}^{M} q_{b,m} \left|\mathbf{g}_{S,b,k}^H \mathbf{w}_{T,b,m}\right|^2 + \sigma_k^2}. \tag{5}$$

The corresponding achievable rates at the k-th SU for the common stream s_0 and the private stream s_k are given by $\mathrm{R}_k^c = \log_2\left(1 + \gamma_k^c\right)$ and $\mathrm{R}_k^p = \log_2\left(1 + \gamma_k^p\right)$, respectively. To ensure that the common stream s_0 can be successful decoded by all the SUs, its rate must not exceed $R_0 = \min\left(R_1^c, ..., R_K^c\right)$. Since R_0 consists of the common parts of the K SU's messages, it can be expressed as $R_0 = \sum\limits_{k=1}^{K} c_k$, where c_k denotes the common rate associated with the k-th user's common message part m_k^c. Hence, the total achievable rate of the k-th SU is defined as $R_k = c_k + R_k^p$.

The interference from the satellite to the m-th TU can be expressed as

$$I_m = \left|\mathbf{h}_{T,m}^H \mathbf{p}_0\right|^2 + \sum_{k=1}^{K} \left|\mathbf{h}_{T,m}^H \mathbf{p}_k\right|^2, \tag{6}$$

where $h_{T,m} \in \mathbb{C}^{N \times 1}$ denotes the channel vector from the satellite to the m-th TU.

For radar sensing, both common and private precoding vectors are used to simultaneously perform target detection and data transmission. The radar sensing performance is evaluated using the transmit beampattern metric, defined as

$$P\left(\theta\right) = \mathbf{a}^H\left(\theta\right) \left(\mathbf{p}_0 \mathbf{p}_0^H + \sum_{k=1}^{K} \mathbf{p}_k \mathbf{p}_k^H\right) \mathbf{a}\left(\theta\right), \tag{7}$$

where $\mathbf{a}\left(\theta\right) = \left[1, e^{j2\pi d_\Delta \sin(\theta)}, ..., e^{j2\pi(N-1)d_\Delta \sin(\theta)}\right]^T$ is the steering vector with direction θ, with d_Δ denoting the normalized spacing between adjacent antenna elements relative to the carrier wavelength. The desired beam pattern is designed to maximize the minimum beampattern gain in the direction of the target, where θ represents the potential target location [4].

Our objective is to maximize the weighted sum rate of the SUs, subject to a power budget constraint at the satellite, a minimum beampattern gain requirement for target sensing, and a maximum allowable interference toward the TUs. The proposed optimization problem is formulated as follows:

$$\max_{\mathbf{p}_0, \mathbf{p}_k, c_k} \quad \sum_{k=1}^{K} u_k \left(R_k^p + c_k\right) \tag{8a}$$

$$\text{s.t. C1: } \sum_{k'=1}^{K} c_{k'} \leq R_k^c, \forall k \tag{8b}$$

$$\text{C2: } P\left(\theta\right) \geq G_{\min} \tag{8c}$$

$$\text{C3: } \left\|\mathbf{p}_0\right\|^2 + \sum_{k=1}^{K} \left\|\mathbf{p}_k\right\|^2 \leq P_{\max} \tag{8d}$$

$$\text{C4: } I_m \leq I_{\max}, \forall m \tag{8e}$$

$$\text{C5: } c_k \geq 0, \forall k, \tag{8f}$$

where u_k denotes the rate weight for the k-th SU, G_{min} represents the minimum beampattern gain in the direction of the target, P_{max} is the satellite's total power budget, and I_{max} is the maximum allowable interference to TUs. Constraint C1 ensures that s_0 can be successfully decoded by all SUs. Constraint C2 enforces the radar requirement by guaranteeing a minimum beampattern gain, while constraint C4 limits the interference introduced to the terrestrial network. The proposed problem (8) is non-convex. To address this, we propose a hybrid solution that combines a deep CNN-based model with an SDR-based method.

III. Proposed Solution

The design of the private precoding vectors $\{\mathbf{p}_1, ..., \mathbf{p}_K\}$ is based on ZF. Then, the private precoding is defined as $\mathbf{p}_k = \alpha_k \frac{\tilde{\mathbf{p}}_k}{\|\tilde{\mathbf{p}}_k\|}$, where α_k^2 represents the transmit power and for ZF, $\tilde{\mathbf{p}}_k$ is the k-th column of $\tilde{\mathbf{P}}_S = \tilde{\mathbf{H}}_S \left(\tilde{\mathbf{H}}_S^H \tilde{\mathbf{H}}_S\right)^{-1} = [\tilde{\mathbf{p}}_1, ..., \tilde{\mathbf{p}}_K] \in \mathbb{C}^{N \times K}$ with $\tilde{\mathbf{H}}_S = [\mathbf{h}_{S,1}, ..., \mathbf{h}_{S,K}] \in \mathbb{C}^{N \times K}$. Next, we divide the non-convex problem (8) into two sub-problems. First, we develop a CNN-based scheme to optimize the power allocation variables $\{\alpha_k\}$. CNNs are particularly well-suited for this task, as the input data consists of complex channel vectors that can be represented as two-channel images, allowing the model to effectively capture spatial patterns and correlations. The CNN model is trained offline using a dataset generated by an SCA-based method. Subsequently, given the power allocation variables $\{\alpha_k\}$ predicted by the trained CNN model, we propose a SDR-based method to optimize the common precoder $\mathbf{p}_0$ and the common rate variables $\{c_k\}$. This hybrid framework not only enables an efficient solution to the original non-convex problem (8), but also improves constraint satisfaction through the SDR module.

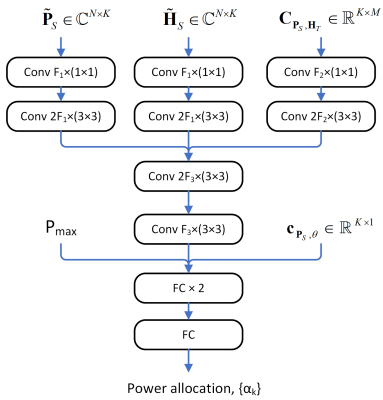

Fig. 2: Proposed CNN-based model for power allocation.

A. CNN-based model to predict $\{\alpha_k\}$.

The proposed CNN-based model is composed of five inputs and one output representing the power allocation variables $\{\alpha_k\}$, as illustrated in Fig. 2. The first input is the ZF based matrix $\tilde{\mathbf{P}}_S$, which consists of real and imaginary components. These components are treated as separate image channels, allowing the matrix to be represented as an image-like input. The second input is the channel matrix $\tilde{\mathbf{H}}_S$ from the satellite to the SUs, which can also be considered as an image with two image channels. The third input is the correlation between private precoders and the channels associated to TUs, defined by $\mathbf{C}_{\mathbf{P}_S,\mathbf{H}_T} = \left|\mathbf{P}_S^H\mathbf{H}_T\right| \in \mathbb{R}^{K\times M}$, where $\mathbf{H}_T = \left[\frac{\mathbf{h}_{T,1}}{\|\mathbf{h}_{T,1}\|},...,\frac{\mathbf{h}_{T,M}}{\|\mathbf{h}_{T,M}\|}\right]$ and $\mathbf{P}_S = \left[\frac{\tilde{\mathbf{p}}_1}{\|\tilde{\mathbf{p}}_1\|},...,\frac{\tilde{\mathbf{p}}_K}{\|\tilde{\mathbf{p}}_K\|}\right]$. The fourth input is the correlation between private precoders, and the steering vector of the angle associated with the direction of the target, which can be represented as $\mathbf{c}_{\mathbf{P}_S,\theta} = \left|\mathbf{P}_S^H\mathbf{a}(\theta)\right| \in \mathbb{R}^{K\times1}$. The last input is the power budget of the satellite.

In Fig. 2, the Conv $w \times (b \times b)$ module is composed of three sequential layers. First, a convolutional layer with w filters and a kernel size of $b \times b$ is applied. This is followed by a batch normalization layer, which accelerates training and enhances stability. Finally, a Parametric ReLU (PReLU) activation function is used to introduce non-linearity, allowing for adaptive learning of the negative slope. The model is trained using the Adam optimizer and compiled with mean squared error (MSE) as both the loss function and evaluation metric, making it well-suited for regression tasks. The Conv module enables feature extraction from complex-valued inputs, effectively capturing and consolidating this information in a high-dimensional feature space. These extracted features are then merged with real-valued inputs, such as power levels and directional correlation toward the target. The combined representation is subsequently passed through three fully connected (FC) layers to generate the power allocation variables $\{\alpha_k\}$.

B. SDR-based method to optimize $\mathbf{p}_0$ and $\{c_k\}$.

In this subsection, we describe the SDR-based method, given the power allocation variables $\{\alpha_k\}$, to optimize $\mathbf{p}_0$ and $\{c_k\}$. First, we define $\mathbf{P}_0 = \mathbf{p}_0\mathbf{p}_0^H$, $\mathbf{H}_{S,k} = \mathbf{h}_{S,k}\mathbf{h}_{S,k}^H$, $\mathbf{H}_{T,m} = \mathbf{h}_{T,m}\mathbf{h}_{T,m}^H$, and $\eta_{k,k'} = \mathbf{h}_{S,k}^H\frac{\tilde{\mathbf{p}}_{k'}}{\|\tilde{\mathbf{p}}_{k'}\|}$. Then, it implies that the matrix $\mathbf{P}_0$ is rank-one symmetric positive semidefinite, i.e., $\mathbf{P}_0 \succeq 0$ and $\mathrm{rank}(\mathbf{P}_0) = 1$. Moreover, the following equivalences hold: $\|\mathbf{p}_0\|^2 = \mathrm{Tr}(\mathbf{P}_0)$, $\left|\mathbf{h}_{S,k}^H\mathbf{p}_0\right|^2 = \mathrm{Tr}(\mathbf{H}_{S,k}\mathbf{P}_0)$, and $\left|\mathbf{h}_{T,m}^H\mathbf{p}_0\right|^2 = \mathrm{Tr}(\mathbf{H}_{T,m}\mathbf{P}_0)$. Then By relaxing the rank-one constraint on $\mathbf{P}_0$, the original non-convex problem (8), given $\{\alpha_k\}$, can be reformulated into a convex optimization problem as follows:

$$\max_{\mathbf{P}_0,c_k} \sum_{k=1}^{K} u_k c_k \tag{9a}$$

subject to

$$-\mathrm{Tr}(\mathbf{H}_{S,k}\mathbf{P}_0) + \left(2^{\sum_{k'=1}^{K} c_{k'}} - 1\right)\left(\sum_{k'=1}^{K}\alpha_{k'}^2|\eta_{k,k'}|^2 + \sum_{b=1}^{B}\sum_{m=1}^{M} q_{b,m}\left|\mathbf{g}_{S,b,k}^H\mathbf{w}_{T,b,m}\right|^2 + \sigma_k^2\right) \le 0,\ \forall k \tag{9b}$$

$$\mathbf{a}^H(\theta)(\mathbf{P}_0)\mathbf{a}(\theta) + \mathbf{a}^H(\theta)\left(\sum_{k=1}^{K}\alpha_k^2\tilde{\mathbf{p}}_k\tilde{\mathbf{p}}_k^H\right)\mathbf{a}(\theta) \ge G_{\min} \tag{9c}$$

$$\mathrm{Tr}(\mathbf{P}_0) + \sum_{k=1}^{K}\alpha_k^2 \le P_{\max} \tag{9d}$$

$$\mathrm{Tr}(\mathbf{H}_{T,m}\mathbf{P}_0) + \sum_{k=1}^{K}\alpha_k^2\left|\mathbf{h}_{T,m}^H\tilde{\mathbf{p}}_k\right|^2 \le I_{\max},\ \forall m \tag{9e}$$

$$\mathbf{P}_0 \succeq 0 \tag{9f}$$

$$c_k \ge 0, \forall k. \tag{9g}$$

Problem (9) is convex and the solution can be obtained by the CVX toolbox in MATLAB [13]. The computational complexity of solving problem (9) can be expressed as $\mathcal{O}\left(\sqrt{N}\left(N^6 + (K+M)N^2\right)\log(1/\zeta)\right)$ [14]. If the predicted values of $\{\alpha_k\}$ result in an infeasible problem, a slack variable s can be introduced into constraint (9d) and incorporated as a penalty term in the objective function to ensure feasibility. Subsequently, the values of α_k are updated based on constraint (9d) using $\mathbf{P}_0^*, s^*$. Moreover, if the optimal $\mathbf{P}_0^*$ to problem (9) is rank-one, the common precoder vector can be obtained by $\mathbf{p}_0 = \sqrt{\lambda_{\max}(\mathbf{P}_0)}\nu_{\max,\mathbf{P}_0}$, where $\lambda_{\max}$ denotes the largest eigenvalue of matrix $\mathbf{P}_0$, and $\nu_{\max,\mathbf{P}_0}$ is the corresponding eigenvector. If $\mathbf{P}_0^*$ is not rank-one, penalty-based optimization approach [15] can be employed to approximate the rank-one matrix constraint, enabling the derivation of near-optimal solutions by progressively enforcing rank-one through penalization.

IV. Simulation Results

Numerical simulations are presented to validate the effectiveness of the proposed scheme. The terrestrial channels from the b-th BS to k-th SU and m-th TU are modelled based on [2] and are defined as $\mathbf{g}_{S(T),b,k(m)} = \sqrt{\alpha_{S(T),b,k(m)}}\tilde{\mathbf{g}}_{S(T),b,k(m)}$, where $\tilde{\mathbf{g}}_{S(T),b,k(m)}$ represents the small-scale fading with elements following $\mathcal{CN}(0,1)$, and $\alpha_{S(T),b,k(m)}$ denotes the large-scale fading coefficient, which accounts for both path loss and shadow fading, as described in [2].

The channel vector from the satellite to k-th SU follows the model described in [12], [9], and is given by $\mathbf{h}_{S,k} = \frac{\sqrt{G_u}}{4\pi\frac{d_{S,k}}{\lambda}\sqrt{\kappa T B_W}}\mathbf{b}_{S,k}^{1/2} \odot \mathbf{r}_{S,k}^{1/2} \odot \exp(j\boldsymbol{\theta}_{S,k})$, where G_u accounts for the antenna gain of the SU, $d_{S,k}$ denotes the distance between the satellite and the k-th SU, λ represents the wavelength, κ=1.38×10^{-23}/K is the Boltzmann's constant, $T = 300$ K is the system noise temperature, and B_W is the bandwidth. The beam gain component is defined as $b_{S,k,n} = G_{Max}\left[\frac{J_1(\delta_{S,k,n})}{2\delta_{S,k,n}} + 36\frac{J_3(\delta_{S,k,n})}{\delta_{S,k,n}^3}\right]^2$, where G_{max} denotes the maximum beam gain, and $J_1(\cdot)$ and $J_3(\cdot)$ are the first- and third-order Bessel functions of the first kind, respectively. $\delta_{S,k,n} = 2.07123\left(\sin(\vartheta_{S,k,n})/\sin(\vartheta_{3dB})\right)$, where $\vartheta_{S,k,n}$ denotes the angle between the n-feed and the k-th SU, and ϑ_{3dB} represents the angle at which the antenna gain is reduced by 3 dB. $\mathbf{r}_{S,k}$ is an N-dimensional vector representing the rain attenuation, and $\boldsymbol{\theta}_{S,k}$ is the channel phase vector with elements independently and uniformly distributed over the interval $[0, 2\pi]$. The channel vector from the satellite to the m-th TU follows the same model.

The LEO satellite is positioned at an altitude of 600 km, located at coordinates $(0, 0)$. SUs are randomly distributed within a circular area of 10 km radius centered at $(0, 0)$. The BSs and TUs are deployed within a 1 km radius area centered at $(12\,\text{km}, 0)$. The BSs are mounted at a height of 15 m, while the TUs are positioned at 1.65 m. SUs are equipped with receiver dishes installed at 10 m. The satellite employs a directional antenna with a maximum gain of 35 dBi and one-half the 3 dB beamwidth of 1.6°, while the satellite receiver achieves 39.74 dBi gain. The system operates at a carrier frequency of 20 GHz with a total bandwidth of 500 MHz. We consider $B = 2$ terrestrial BSs, each equipped with $N_B = 4$ antennas and transmitting at 25 dBm. The transmit power is equally divided among $M = 2$ served TUs. The satellite is equipped with $N = 4$ antennas, serving $K = 2$ SUs with $u_k = 1$, and operates with a power budget ranging from 30 dBm to 36 dBm. An interference-to-noise ratio (I/N) threshold of -10 dB is considered at the TUs.

We compare the proposed hybrid CNN-SDR scheme, referred to as "RSMA-CNN", with the near-optimal SCA-based method [10], [14], denoted as "RSMA-SCA", which iteratively solves the non-convex problem (8) by constructing and solving a sequence of convex approximations. Additionally, we consider RSMA without radar constraints, denoted as "RSMA w/o radar", as well as two baseline schemes based on ZF and MRT, which optimize the power allocation for user precoders and the complex precoding vector of the dedicated radar signal.

The RSMA-SCA method was employed to generate the dataset used for training the deep CNN model, comprising 32,000 training samples and 8,000 validation samples. After fine-tuning, the selected model parameters include $F_1 = 8$, $F_2 = 4$, $F_3 = 64$, 1024 hidden neurons in the FC layers, a batch size of 128, and an initial learning rate of lr with a exponential decay factor of 0.95 applied every 1,000 mini-batch updates. Fig. 3a illustrates the convergence behavior of

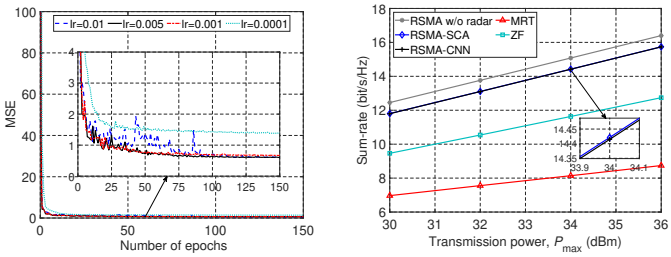

(a) (b)

Fig. 3: (a) Convergence behavior of the CNN-based model. (b) Sum-rate versus the transmission power.

the proposed deep CNN-based scheme under different learning rates. It can be observed that relatively high learning rate values lead to unstable MSE behavior. In contrast, lower learning rates result in higher final MSE values. Therefore, a learning rate of $lr = 0.005$ is selected for training the final model, as it provides a good balance between stability and performance.

Fig. 3b presents the sum-rate performance according to the power budget at the LEO satellite. We can see that RSMA-based schemes outperform the baseline methods of ZF and MRT, owing to the ability of RSMA to partially decode both radar and inter-user interference through the common stream. RSMA w/o radar achieves a slight improvement in sum-rate compared to the proposed RSMA with radar, owing to the additional radar constraints (8c) that restrict its communication performance. Notably, the proposed hybrid CNN-SDR scheme achieves 99.9% of RSMA-SCA's sum-rate with significantly lower computational complexity.

Fig. 4a illustrates the cumulative distribution function (CDF) of the sum-rate over multiple channel realizations, considering power budgets of $P_{\max} = 32$ dBm and $P_{\max} = 36$ dBm. The results show that the proposed hybrid CNN-SDR scheme closely matches the performance of the RSMA-SCA method for different channel realizations, demonstrating its effectiveness in achieving near-optimal power allocation and precoding. Moreover, the RSMA-based schemes consistently outperform the baseline methods of ZF and MRT.

Fig. 4b presents the normalized transmit beampattern obtained for the target with $P_{max} = 30$ dBm, where the angle $\theta^* = 0^\cdot$ is selected for improved visualization. The transmit beampattern is normalized with respect to the minimum required beampattern gain, G_{min}. It can be observed that the RSMA-SCA and RSMA-CNN schemes yield comparable performance in satisfying the radar requirement. Additionally, the baseline methods of ZF and MRT exhibit similar beampattern characteristics to the RSMA-based schemes. This is attributed to the radar constraint (8c), which enforces a minimum beampattern gain while allowing the remaining resources to be allocated for maximizing the users' sum-rate.

Fig. 4c shows the CDF of the computational time required by each comparative scheme. All simulations were conducted

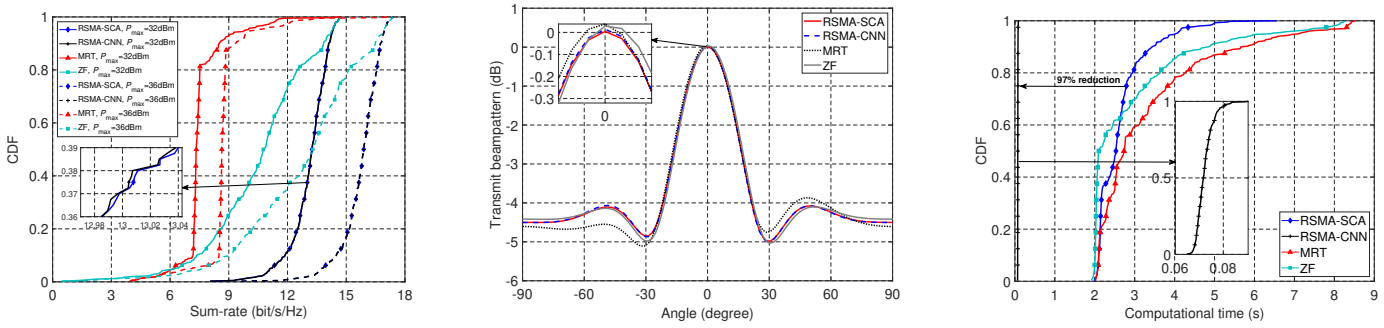

(a) (b) (c)

Fig. 4: (a) CDF of the sum-rate. (b) Normalized transmit beampattern for a target with $\theta^* = 0^{\cdot}$. (c) CDF of the computational time.

on a workstation equipped with an Intel Core i9-14900K processor and 64 GB of RAM. The computational time for the proposed method includes both the CNN-based model and the SDR-based technique, with the CNN inference averaging 4.3 ms when executed solely on the CPU to ensure a fair comparison with the baseline methods. The iterative baseline schemes are considered converged when the relative change in the objective function between successive iterations falls below 10^{-4}. Our proposed hybrid CNN-SDR scheme achieves an average 97.3% reduction in computational time compared to the RSMA-SCA method. It also achieves 97.5% and 97.8% reductions relative to the ZF and MRT baselines, respectively, both of which involve radar precoding vector optimization. These results highlight the superior computational efficiency and overall performance of the proposed approach.

V. Conclusion

In this paper, we have proposed a RSMA-based cognitive satellite–terrestrial network architecture that enables a multi-antenna LEO satellite to perform joint communication and sensing while sharing spectrum with a terrestrial distributed MIMO system. We investigated the weighted sum-rate maximization problem under power, sensing, and interference constraints, and proposed a hybrid CNN-SDR solution that leverages deep learning for power allocation alongside SDR-based common precoding and rate optimization. Simulation results confirmed that the proposed scheme achieved performance close to a SCA-based benchmark, satisfied all system constraints, and significantly reduced computational complexity. Furthermore, the RSMA-based approach consistently outperformed conventional baseline schemes, demonstrating its viability as a practical solution for future integrated satellite–terrestrial networks.

References

[1] G. Geraci, D. López-Pérez, M. Benzaghta, and S. Chatzinotas, "Integrating Terrestrial and Non-Terrestrial Networks: 3D Opportunities and Challenges," *IEEE Commun. Mag.*, vol. 61, no. 4, pp. 42–48, Apr. 2023.

[2] H. Q. Ngo, A. Ashikhmin, H. Yang, E. G. Larsson, and T. L. Marzetta, "Cell-Free Massive MIMO Versus Small Cells," *IEEE Trans. Wireless Commun.*, vol. 16, no. 3, pp. 1834–1850, Mar. 2017, doi: 10.1109/twc.2017.2655515.

[3] F. Riera-Palou, G. Femenias, M. Caus, M. Shaat, and A. I. Perez-Neira, "Scalable Cell-Free Massive MIMO Networks With LEO Satellite Support," *IEEE Access*, vol. 10, pp. 37557–37571, 2022

[4] H. Hua, J. Xu, and T. X. Han, "Optimal Transmit Beamforming for Integrated Sensing and Communication," *IEEE Trans. Veh. Technol.*, vol. 72, no. 8, pp. 10588–10603, Aug. 2023.

[5] Y. Mao, B. Clerckx, and V. O. K. Li, "Rate-splitting multiple access for downlink communication systems: bridging, generalizing, and outperforming SDMA and NOMA," *EURASIP J. Wirel. Commun. Netw.*, vol. 2018, no. 1, p. 133, May 2018.

[6] C. Xu, B. Clerckx, S. Chen, Y. Mao, and J. Zhang, "Rate-Splitting Multiple Access for Multi-Antenna Joint Radar and Communications," *IEEE J. Sel. Top. Signal Process.*, vol. 15, no. 6, pp. 1332–1347, Nov. 2021.

[7] L. Yin, Z. Liu, M. R. B. Shankar, M. Alaee-Kerahroodi, and B. Clerckx, "Integrated Sensing and Communications Enabled Low Earth Orbit Satellite Systems," *IEEE Netw.*, vol. 38, no. 6, pp. 252–258, Nov. 2024.

[8] B. Zhao, M. Wang, Z. Xing, G. Ren, and J. Su, "Integrated Sensing and Communication Aided Dynamic Resource Allocation for Random Access in Satellite Terrestrial Relay Networks," *IEEE Commun. Lett.*, vol. 27, no. 2, pp. 661–665, Feb. 2023.

[9] S. Pala, K. Singh, C.-P. Li, and O. A. Dobre, "Empowering ISAC Systems With Federated Learning: A Focus on Satellite and RIS-Enhanced Terrestrial Integrated Networks," *IEEE Trans. Wireless Commun.*, vol. 24, no. 1, pp. 810–824, Jan. 2025.

[10] M. R. Camana, Z. Abdullah, C. E. Garcia, E. Lagunas, and S. Chatzinotas, "Rate-Splitting Multiple Access for a Multi-RIS-Assisted Cell-Free Network with Low-Resolution DACs," in 2025 IEEE Wireless Communications and Networking Conference (WCNC), pp. 1–6, Mar. 2025.

[11] Z. Wang, R. Ma, H. Shi, Z. Cai, L. Lin, and H. Guan, "Deep Convolutional Linear Precoder Neural Network for Rate Splitting Strategy of Aerial Computing Networks," *IEEE Trans. Netw. Sci. Eng.*, vol. 11, no. 6, pp. 5228–5243, Nov. 2024.

[12] J. Chu, X. Chen, C. Zhong, and Z. Zhang, "Robust Design for NOMA-Based Multibeam LEO Satellite Internet of Things," *IEEE Internet Things J.*, vol. 8, no. 3, pp. 1959–1970, Feb. 2021.

[13] M. C. Grant and S. P. Boyd. "CVX: MATLAB Software for Disciplined Convex Programming, Version 2.2." Jul. 2024. [Online]. Available: http://cvxr.com/cvx

[14] C. E. Garcia, M. R. Camana, J. Querol, and S. Chatzinotas, "Rate-Splitting Multiple Access for Secure Communications Over CR MISO SWIPT Systems With Non-Linear EH Users," *IEEE Trans. Green Commun. Netw.*, vol. 8, no. 4, pp. 1332–1347, Dec. 2024.

[15] A. H. Phan, H. D. Tuan, H. H. Kha, and D. T. Ngo, "Nonsmooth optimization for efficient beamforming in cognitive radio multicast transmission," *IEEE Trans. Signal Process.*, vol. 60, no. 6, pp. 2941–2951, Jun. 2012.